Adsorption of Hexadecyltrimethylammonium Bromide to Mica: Nanometer-Scale Study of Binding-Site Competition Effects

ARTICLE *in* LANGMUIR · DECEMBER 1998

Impact Factor: 4.46 · DOI: 10.1021/la9710942

2 AUTHORS:

William Ducker
Virginia Tech
124 PUBLICATIONS **6,600** CITATIONS
SEE PROFILE

Erica J Wanless
University of Newcastle
81 PUBLICATIONS **2,512** CITATIONS
SEE PROFILE

Adsorption of Hexadecyltrimethylammonium Bromide to Mica: Nanometer-Scale Study of Binding-Site Competition Effects

William A. Ducker* and Erica J. Wanless†

Department of Chemistry, University of Otago, P.O. Box 56, Dunedin, New Zealand, and Department of Chemistry, Virginia Tech, Blacksburg, Virginia

Received October 7, 1997. In Final Form: October 29, 1998

We have changed the structure of an adsorbed surfactant layer by modifying the nature of the interface *in situ*. Muscovite mica contains surface anions that can bind to a variety of cations in aqueous solution. Using an atomic force microscope (AFM), we have investigated the influence of the adsorption of the salts HBr, KBr, and $N(CH_2CH_3)_4Br$ on the adsorption of hexadecyltrimethylammonium bromide (CTAB) to mica. In the absence of salt, at twice the bulk critical micelle concentration, CTAB initially forms cylindrical surface micelles on mica. The cylinders transform to a flat bilayer structure within 24 h. The introduction of 10 mM K^+ produces cylindrical aggregates that are stable, and a further increase in the concentration of K^+ produces defects in the cylinders. These defects consist of aggregate termini and changes in the direction of the long axis of single aggregates. More defects are introduced by H^+ than by K^+ (at the same concentration). This is consistent with the known higher binding constant of H^+ to mica. Using the introduction of defects as an indicator of the adsorption of cations in the presence of CTA^+, we find that CTAB greatly slows adsorption of H^+ but that the speed of K^+ adsorption is not noticeably affected. The adsorption of K^+ produces structures that are sensitive to the force that is applied by the AFM tip. At a critical repulsive force, the image changes discontinuously from a defective cylinder structure to a spherical or flattened disklike structure.

Introduction

An important property of surfactants is that they partition to an interface. The result of this partitioning is that surfactants can be used to modify interfacial properties at very low bulk concentrations, and thus surfactants change interfacial properties cheaply. Another important property of surfactants is that they form organized structures such as micelles and vesicles in bulk solution. Recently it has been demonstrated that adsorbed surfactants also display distinct organization at interfaces.[1] Work is now underway to systematically study the relationship between the forces acting on individual surfactants and the shape of the adsorbed surfactant aggregate.

The positioning of surfactant at an interface between water and another phase (in this work, a mineral) is the result of an energy minimization for the surfactant, the water, and the surface of the mineral. Some of the important contributions to this energy are as follows:

(1) Interactions between the surfactant and the mineral surface. The hydrophilic and/or the hydrophobic portion must be attracted to the interface.

(2) Interactions between the water and the mineral surface. A weak interaction will promote surfactant adsorption.

(3) Interactions between the surfactant tail groups and water. This interaction is weaker than the interaction between water molecules, so it promotes surfactant aggregation both in bulk solution and at interfaces.

Considering contributions 1 and 2 together, we note that the surfactant must displace water from the mineral surface. Thus, a higher energy mineral surface drives the surfactant to form a more continuous film on the mineral surface.[2]

In this work we studied the shape of the aggregates of the cationic surfactant hexadecyltrimethylammonium bromide (CTAB) adsorbed to the muscovite mica/aqueous solution interface in order to examine the role of electrostatic interactions on surface aggregation. When muscovite mica is placed in solution, the K^+ ions from the basal plane desorb and exchange with other ions. Electrokinetic[3] and surface forces apparatus (SFA)[4,5] measurements have been used to measure the surface potential of mica in a variety of electrolyte solutions, and XPS[6] has been used to identify the adsorption density of competing ions. These measurements have been used to describe the ion-exchange properties of mica in terms of surface equilibria:

$$SM \rightleftarrows S^- + M^+_{surface}$$

where S represents the mica surface site, M^+ is a cation, and SM is a cation bound to the mica surface. The equilibrium constants pK_M for this surface reaction are 6, 3.5, 3.8, and 3.1, respectively, for H^+, K^+, $N(CH_3)_4^+$, and NH_4^+;[3,7,8] that is, the proton is much more strongly bound than other small cations. If we know the equilibrium

* For correspondence: Department of Chemistry, Virginia Tech.
† Now at Department of Chemistry, University of Newcastle, Newcastle, Australia.

(1) Manne, S.; Cleveland, J. P.; Gaub, H. E.; Stucky, G. D.; Hansma, P. K. *Langmuir* **1994**, *10*, 4409−4413.
(2) Grant, L. M.; Tiberg, F.; Ducker, W. A. *J. Phys. Chem.* **1988**, *102*, 4288−4294.
(3) Scales, P. J.; Grieser, F.; Healy, T. W. *Langmuir* **1990**, *6*, 582−598.
(4) Kékicheff, P.; Christenson, H. K.; Ninham, B. W. *Colloids Surf.* **1989**, *40*, 31−41.
(5) Claesson, P.; Horn, R. G.; Pashley, R. M. *J. Colloid Interface Sci.* **1984**, *100*, 250−263.
(6) Claesson, P. M.; Herder, P.; Stenius, P.; Eriksson, J. C.; Pashley, R. M. *J. Colloid Interface Sci.* **1986**, *109*, 31−39.
(7) Pashley, R. M. *J. Colloid Interface Sci.* **1981**, *83*, 531−546.
(8) Ducker, W. A.; Pashley, R. M. *J. Colloid Interface Sci.* **1989**, *131*, 433.

10.1021/la9710942 CCC: $18.00
Published on Web 12/04/1998

constant, the surface potential, and the bulk ion concentration, we can use these constants to determine the surface concentrations of each species. When CTAB adsorbs to mica, it is reasonable to assume that there is an electrostatic contribution due to bonding of the quaternary ammonium group to the negative mica lattice charge. However, it is unlikely that the binding constant is independent of the surfactant surface concentration because the free energy contribution from the surfactant tail depends on whether it neighbors surfactant or water molecules. The dependence of the surfactant adsorption energy on the surroundings leads to association but prevents us from making a simple mass-action analysis. However, by comparison of adsorption in the presence of different cations of known binding constant, we can make conclusions about the contribution of ion binding to surfactant arrangements.

We can change the density of surface-binding sites that are available to the surfactant headgroups by varying the bulk concentration of cations (H^+ or K^+), and thereby examine the effect of the density of surface sites on the shape of surfactant aggregates. Previously, it has been reported that KBr causes a shift in the properties of CTAB on mica to those of a more dilute CTAB solution in the absence of KBr.[4] This suggests that there is competition between K^+ and CTA^+ for surface sites. Chen et al. have used X-ray photoelectron spectroscopy (XPS) to measure the density of cations remaining on mica after the mica is equilibrated in a CTAB/salt solution and then dried in air followed by high vacuum.[9] They find that the density of CTA^+ slowly rises and the density of rival cations slowly falls over a period of several days. This slow change was attributed to the barrier that the surfactant film provides to diffusion of ions to the mica surface. In a recent publication, we have found that, for CTAB-only solutions, there is a change from cylindrical aggregates to a flat sheet on mica over a period of about 1 day.[10]

Previously it has also been shown that, at about 2 × cmc, both tetradecyltrimethylammonium bromide (TTAB)[11] and dodecyltrimethylammonium bromide (DTAB)[12] adsorb to mica in the form of aggregates in which one axis is approximately equal to the diameter of a micelle and the other is very long. (The DTAB was equilibrated for about 2 h, but there is no record of the equilibration of the TTAB.) The long axes are all aligned in a single direction. The solution micelles in equilibrium with these surface micelles are approximately spherical, so the effect of the mica surface is to produce a lower curvature aggregate. In a solution micelle, the separation between quaternary ammonium groups is a compromise between electrostatic repulsion and attraction due to exposure of the hydrophobic interior. The headgroup area for CTAB in a micelle is about 0.64 nm^2.[13] The surface of mica has one negative site[14] per 0.48 nm^2, so when surfactant adsorbs, the density of potential surfactant counterions is greater on the mica surface than in a micelle. It is reasonable to expect that this increase in counterion density on the mica surface will lead to screening of the repulsive electrostatic forces between the CTA^+ headgroups and thus to a lower curvature aggregate such as a cylinder or flat sheet on the mica surface.[15] (This hypothesis has recently been used to describe the adsorption of gemini surfactants.[16]) Since the mica counterion sites are fixed by the crystallography, the alignment of the aggregates may be fixed in relation to the mica crystal axes. Also, the mica lattice ions are confined to a plane, which should template a planar aggregate. If cations are introduced to compete for surface sites, then this model predicts that the cylindrical structure should be interrupted by an adsorbed cation. That is, cations will introduce defect structures (Figure 1).

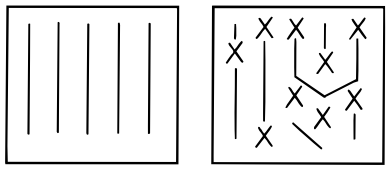

Figure 1. (left) Attachment of surface aggregates via crystalline substrate features may lead to oriented surface aggregates. (right) Occupation of adsorption sites by rival ions may lead to interruption of the ordered structure.

The attraction of surfactant molecules to the dissociated mica lattice sites also leads to an increase in the density of aggregates at the surface relative to bulk solution. A clear manifestation of this is the fact that surface aggregates can occur in equilibrium with a solution that is below the cmc (at about $^1/_3$ × cmc for SDS on graphite[17] and $^1/_2$ × cmc for CTAB on mica[18]). Because the surface micelles are more concentrated than the equilibrium bulk micelles, micelle−micelle interactions will be more important in determining the shape of surface micelles. These micelle−micelle interactions are another factor that may lead to differences between surface and bulk structures.

In this paper we test the effect of H^+, K^+, and $N(CH_2CH_3)_4^+$ on the adsorption of CTA^+ to the surface of mica at a constant 1.8 mM CTA^+ (2 × cmc in the absence of salt[19]). The addition of electrolyte decreases the cmc, so all experiments are above the cmc. We use CTAB because previous work provides us with the surface potential and binding constants and tells us that the thickness of the adsorbed CTAB layer is between 3.1 and 3.5 nm[3], that is, that it is a bit less than twice the extended length of a CTAB molecule. Cryotransmission electron microscopy (TEM) experiments[20] show that addition of salt and surfactant to CTAB solutions causes a change in surfactant aggregate structure in bulk solution. Near the cmc, CTAB forms spherical micelles; at 8 mM CTAB and 300 mM NaBr, the micelles are wormlike. The transition to wormlike micelles was rationalized by assuming that the introduction of salt reduces headgroup−headgroup repulsions.

Experimental Section

Sample Preparation and Characterization. Water was distilled and then passed through a Milli-Q RG system consisting of charcoal filters, ion-exchange media, and a 0.2 μm filter. The resulting water had a conductivity of 18 MΩ cm^{-1} and a surface tension of 72.4 mJ m^{-2} at 22.0 °C.

(9) Chen, Y.-L.; Chen, S.; Frank, C.; Israelachvili, J. *J. Colloid Interface Sci.* **1992**, *153*, 244−265.
(10) Lamont, R. E.; Ducker, W. A. *J. Am. Chem. Soc.* **1998**, *120*, 7062−7067.
(11) Manne, S.; Gaub, H. E. *Science* **1995**, *270*, 1480−1482.
(12) Ducker, W. A.; Wanless, E. J. *Langmuir* **1996**, *12*, 5915−5919.
(13) Warr, G. G.; Radha, S.; Evand, D. F.; Trend, J. E. *J Phys. Chem.* **1998**, *92*, 774−783. (Calculated from the aggregation number assuming spherical micelles.)
(14) Gains, G. L.; Tabor, D. *Nature* **1956**, *178*, 1305−1306.
(15) Ducker, W. A.; Grant, L. M. *J. Phys. Chem.* **1996**, *100*, 11507−11510.
(16) Manne, S.; Schäffer, T. E.; Huo, Q.; Hansma, P. K.; Morse, D. E.; Stucky, G. D.; Aksay, I. A. *Langmuir* **1997**, *13*, 6382−6387.
(17) Wanless, E. J.; Ducker, W. A. *J. Phys. Chem.* **1996**, *100*, 3207−3214.
(18) Lamont, R. Private communication.
(19) Ray, A. *J. Am. Chem. Soc.* **1969**, *91*, 6511. (We find the same cmc by NMR.)
(20) Vinson, P. K.; Bellare, J. R.; Davis, H. T.; Miller, W. G.; Scriven, L. E. *J. Colloid Interface Sci.* **1991**, *142*, 74−91.

Hexadecyltrimethylammonium bromide, 99% (BDH, Poole, U.K.), was recrystallized three times from a distilled-acetone/water mix. Elemental analysis of the purified surfactant showed the correct elemental ratios within the error of the technique (±0.4%). There was no minimum in a plot of surface tension as a function of concentration. KBr (98.5%) and HBr (47%) were used as purchased from BDH.

Microscopy. Images were captured using a Nanoscope III AFM (Digital Instruments, CA) using silicon ultralevers (Park Scientific, CA) with spring constants of 0.12 ± 0.02 N m^{-1}, as determined by measuring the resonant frequency of loaded and unloaded cantilevers.[21] The ultralevers were irradiated for 40 min (~9 mW/cm^2 at 253.7 nm) in a laminar flow cabinet before use. Unless otherwise stated, the images presented are deflection images (showing the error in the feedback signal) with low integral and proportional gains and scan rates of about 10 Hz. No filtering of images was performed other than that inherent in the feedback loop. Distances in lateral dimensions were calibrated by imaging a standard grid (2160 lines/mm), and distances normal to the surface were calibrated by measuring etch pits (180 nm deep).

All measurements were performed in the temperature range 25 ± 2 °C and in equilibrium with single-phase surfactant solutions. The 1-mW laser used to detect the bending of the cantilever has a minimal effect on the temperature of the sample under the cantilever. When a thermistor is imaged in water, the temperature of the thermistor rises by only 0.1 °C when the laser is turned on. Before the images were captured, the mica substrate was left to equilibrate in the solution of interest for at least 30 min, unless stated otherwise. The interface was then monitored for at least 2 h in each solution. Solutions were changed by flushing the AFM cell with about 20 times its volume of new solution over 5 min. For the quickly adsorbing surfactant and the concentrations used here, this meant that the cell equilibrium concentration was very close to that of the flushing solution. Imaging was performed at a repulsive force with the tip separated from the mica by about 3−4 nm. Under this condition the force on the tip is dominated by the surfactant film and thus the image provides information about the surfactant film.

The forces between the tip and sample were also measured using a Nanoscope III AFM and analyzed as described previously.[22] It is important to note that the zero of distance is defined to occur when the gradient of the force has a high and constant (negative) value, which implies that the tip is in contact with the sample. Very strongly adsorbed material may not be displaced in a particular measurement, and therefore there may be a systematic error in evaluating the zero of separation for each complete measurement of force as a function of separation. The zero of force is defined to occur when the gradient in force is very low at a large separation.

Results

Initial Adsorption from CTAB-Only Solution. The initial structure of CTAB aggregates adsorbed to the interface between muscovite mica and a 1.8 mM CTAB solution (2 × cmc) is shown in Figure 2a. These structures are stable for several hours. The aggregates have one long axis and one short axis. The long axes of all the aggregates are aligned roughly parallel over large areas of the sample (>10 μm)^2. Along any aggregate, the long axis wanders up to about 10° from the average direction. Recently, Sharma et al.[23] imaged the same system. Their results indicate lateral organization on a 100 nm scale. Our results do not show aggregation on such a scale; instead, we observe features that are about 7 nm in diameter.

The force between the (oxide coated) silicon tip and the mica is shown in Figure 2b; a long-range repulsive force decays exponentially at separations greater than about 10 nm. The decay length is 7 nm, which is the decay length expected for a double-layer interaction in 1.8 mM 1:1 electrolyte, even though the solution is above the cmc and thus we do not have a 1:1 electrolyte. A similar repulsive electrostatic force in the plane of the interface probably contributes to the alignment of the long axis of the aggregates. There is a mechanical instability at a separation of 3.5−4.5 nm (4.2 nm in Figure 2b), which is probably due to displacement of the surfactant layer. This separation is larger than the thickness of a CTAB layer on mica measured by the surface forces apparatus.[4] The discrepancy could be due to simultaneous desorption of surfactant

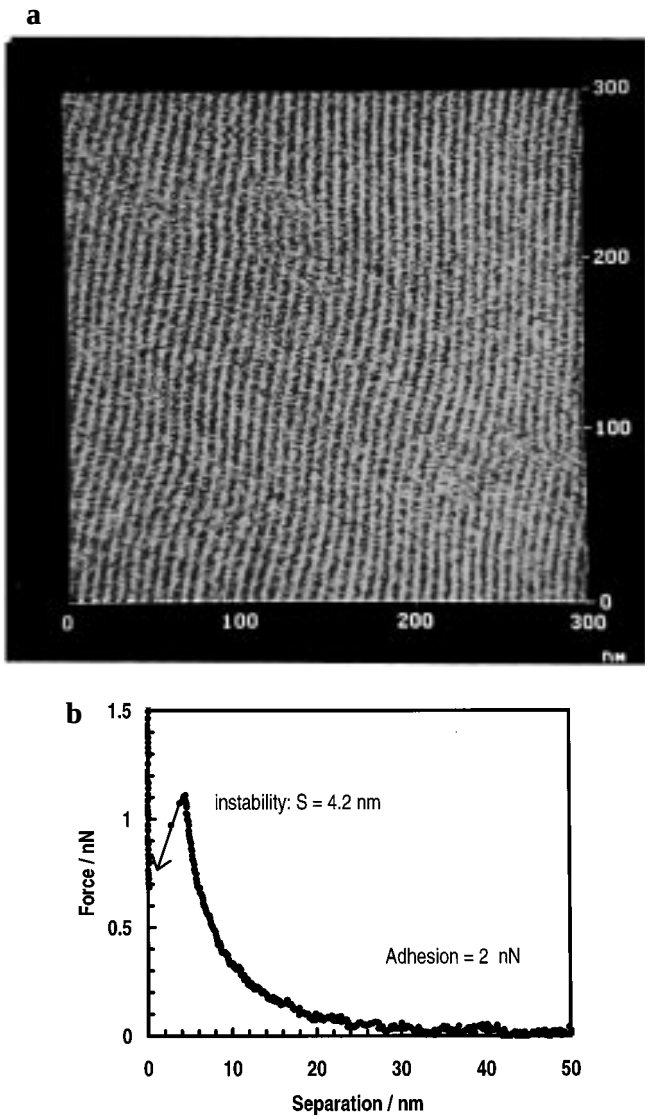

Figure 2. (a) AFM image of the interface between aqueous 1.8 mM CTAB solution and muscovite mica showing the initial organization of the surfactant into long cylinders. (Image captured 2 h after exposure.) After 24 h, AFM images show no features, suggesting that the adsorbed layer is a bilayer. (b) Force between a silicon AFM tip and mica in 1.8 mM CTAB solution. The approach of the tip is reversible up to the load at which the mechanical instability occurs (The instability is marked by the arrow). The image in part a was captured at a slightly lower force (greater separation) than that required for instability. After the instability, a negative load of 2 nN must be applied to increase the separation between the tip and the mica. In some experiments there was an additional small instability at a lower force. This may be due to the attractive van der Waals forces. When the surface film transforms to a bilayer, the force curve is very similar, except that a greater barrier is observed before the instability.

(21) Cleveland, J. P.; Manne, S.; Bocek, D.; Hansma, P. K. *Rev. Sci. Instrum.* **1993**, *64*, 403−405.
(22) Ducker, W. A.; Senden, T. J.; Pashley, R. M. *Langmuir* **1992**, *8*, 1831−1836.
(23) Sharma, B. G.; Basu, S.; Sharma, M. M. *Langmuir* **1996**, *12*, 6506−6512.

from the AFM tip or because it is easier to displace the CTAB aggregates with a sharp AFM tip than with a large flat mica sheet.

If the force applied by the measurement spring is decreased before the instability, then the force is reversible. However, once the force exceeds this critical magnitude, a negative load is required to separate the tip from the surface (the interaction is adhesive). The absolute magnitude of the force (including the adhesion) varies by up to a factor of 10 from experiment to experiment when different tips are used.

The shape of the force map recorded in the AFM image, the thickness of the layer, and energetic considerations suggest that the initial state of the adsorbed CTAB aggregates is cylindrical, as proposed previously for CTAB in 0.14 mol L^{-1} solution.[24] The repeat unit for the observed structure is about 7 nm. This is longer than twice the extended length of a CTA^+ molecule, so if we assume that there is no empty space or water inside the aggregate, then either the aggregates must be flattened cylinders or there must be a water gap between aggregates. Both ideas have some merit. It is likely that the cylinders are somewhat flattened on the mica side to bring the cationic headgroups into close proximity with the negative lattice sites, and electrostatic repulsion between neighboring aggregates should keep the aggregates apart.

Equilibrium Adsorption from CTAB-Only Solution. When the adsorbed structure was monitored again after 17−25 h of equilibration, the structure had changed from cylinders to a flat sheet; that is, there was no measurable variation in force as the AFM tip was scanned across the interface. The thickness measurements performed here and in previous SFA studies,[4,25] and the idea that some headgroups should bind to mica and others should be in contact with solution, suggest that this is a bilayer. A bilayer structure was assumed in the original SFA papers. The slow change from cylinders to a bilayer is consistent with the XPS results (of Chen et al.[9]), which showed a slow increase in the density of CTA^+ molecules at the mica surface.

Adsorption from CTAB and KBr Solutions. When adsorption occurs from a solution that is 1.8 mM KBr and 1.8 mM CTAB, the results are the same as those for pure CTAB solutions, that is, initial adsorption of cylinders and equilibrium adsorption of a flat sheet. Transformation to the flat sheet occurs within about 18 h of exposure of the mica to the solution. Adsorption from 10 mM KBr/1.8 mM CTAB also initially produced cylindrical structures, but these cylinders were then stable. Figure 3a shows the final structure of adsorbed CTAB aggregates in the presence of 10 mM KBr. Figure 3b shows the molecular structure that is consistent with both the AFM image and the repulsive force curve that is measured between the tip and sample. These cylindrical aggregates formed in salt solution were much easier to image than those initially formed in CTAB-only solutions. This could be either because the cylinders are more curved or better formed or simply because the salt reduces the magnitude and decay length of the double-layer force. A higher force gradient should allow greater resolution, and this should be achieved with no double-layer force (using the hydration/protrusion force) or with a very rapidly decaying double-layer force. In 10 mM KBr, the image was also pressure sensitive, as described below.

Figure 4 shows measurements in 1.8 mM CTAB and 101 mM KBr. The observed image was strongly dependent on the measurement force, which is shown in Figure 4a. The imaged structure and the tip−mica force−distance curve is divided into three regimes by the two mechanical instabilities shown in Figure 4a. For different experiments, there was significant variation in the relative force at which these instabilities occurred, and sometimes only one large instability was recorded. The three corresponding states are shown in Figure 4b, which is an image captured while the force was increased in small increments. At low force (Figure 4c and d) the structure is cylindrical, but with more defects (such as termini and changes in the direction of the long axis) than in 10 mM KBr. Ordered arrays of cylinders typically cover less than $(30-50\ \text{nm})^2$ of the mica. The surface also appears to be "lumpy": there are high and low patches extending over

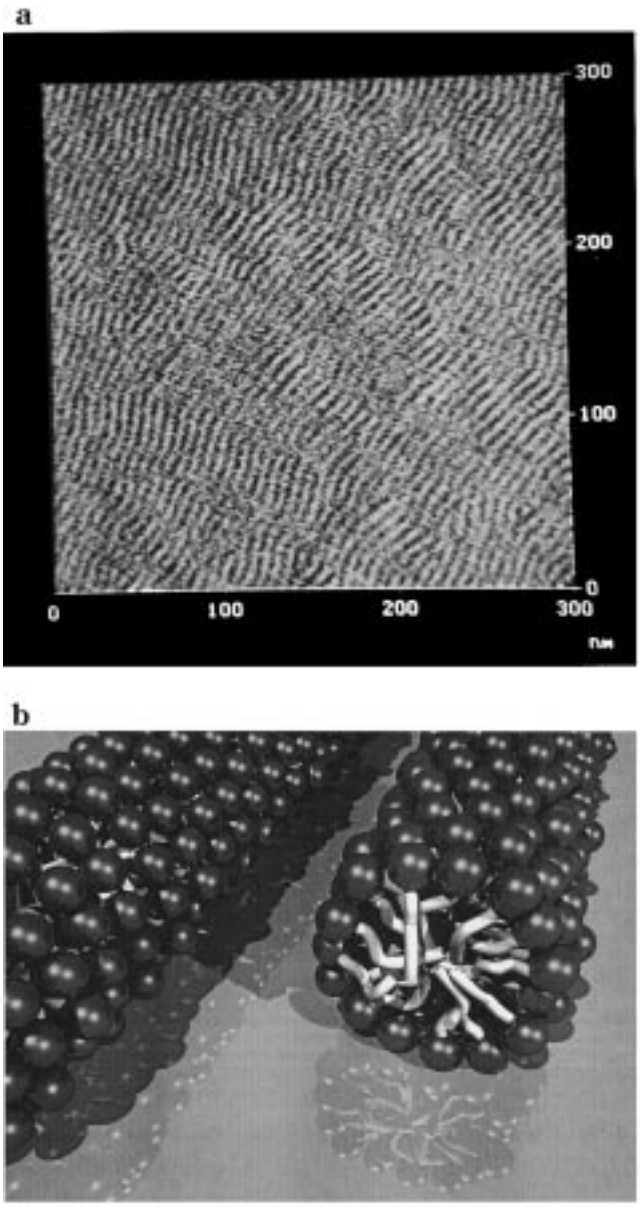

Figure 3. (a) AFM image of the interface between aqueous 1.8 mM CTAB solution and muscovite mica in 10 mM KBr. The surface film is produced immediately on exposure of the mica and does not change with time (up to 30 h). (b) Schematic representation of the cylindrical structure of CTAB adsorbed to the mica surface in 10 mM KBr. Part of the structure on the right has been cut away to reveal the interior. The cylinders may be flattened on the bottom because of an attractive electrostatic force with the mica. This structure is also formed on mica in the early stages of adsorption from 1.8 mM CTAB-only solution.

(24) Reiss-Husson, F.; Luzzati, V. *J. Phys. Chem.* **1964**, *68*, 3504−3511.

(25) Pashley, R. M.; Israelachvili, J. N. *Colloids Surf.* **1981**, *2*, 169.

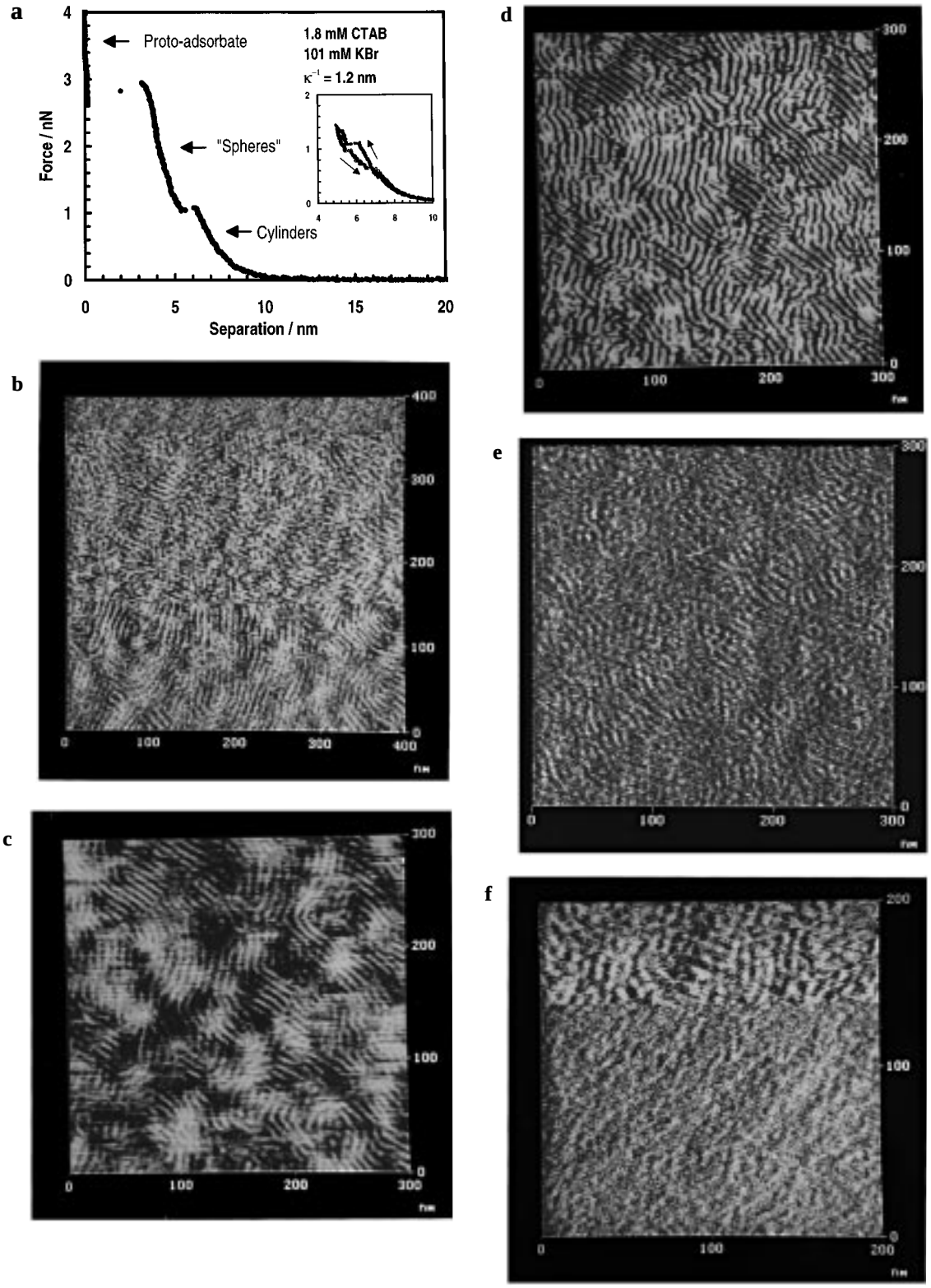

Figure 4. 1.8 mM CTAB and 101 mM KBr. (a) The force between a silicon oxide tip and the mica surface. Three distinct regimes are labeled according to the structure observed at that force in the AFM image. The inset shows that the path of the tip is almost reversible after the low-force (1 nN) instability. The shape of the force curve between the instabilities was somewhat variable, and there was a much larger adhesion (2.5 nN) after the high-force (3 nN) instability. (b) AFM image in which the force was gradually increased going up the image. Although the force was increased gradually, the image changes discontinuously between the regimes marked in part a. The observed structures are cylinders at low force, spheres at moderate force and the proto-adsorbate at higher force. (c) $(300\ nm)^2$ AFM image showing the structure at low force. There are many more defects than at lower concentrations of KBr. In particular the aggregate axis no longer has a uniform orientation: there are now two preferred directions. There is also a roughly even distribution of high points (separated by about 50 nm), which are not always associated with changes in the aggregate direction. (d) Height image captured simultaneously to part c but high pass filtered to clearly show the aggregate defects. (e) Structure of the adsorbate at moderate force showing that the two axes parallel to the interface are much closer in length than at low force. (f) Deflection image of the transition from the spherical structure (top) to the "proto-micelle" structure (bottom). The entire image was captured at the same feedback force of approximately +3 nN.

about 5 aggregate diameters. The massive disordering on addition of K^+ is consistent with a model in which K^+ disrupts the surfactant structure by competing with CTA^+ for negative mica lattice sites. Fourier transforms of these images show that the cylinders are not randomly oriented but are preferentially oriented in one or two or, less often, in three or four directions.

When the force is increased (beyond ~1 nN in Figure 4a), the shape of the adsorbate changes discontinuously. At this force the two axes of the imaged features are approximately equal; that is, the aggregates appear to be spherical (Figure 4e). At higher force (~3 nN in Figure 4a) there is another mechanical instability in the force curve and the image becomes much smoother (Figure 4f). There is little subsequent change in structure at higher forces.

The cylinder to sphere transition is an interesting phenomenon; it may be the first evidence of a pressure-induced phase transition in a thin film. A slight increase in force causes the tip to move about 0.8 nm closer to the mica surface, still leaving 3−5 nm of thin film. Before we attribute this observation to a morphological transformation of the film, we should consider possible alternative explanations. One alternate explanation is that there are actually two layers of surfactant aggregates, both spheres and cylinders, and that the tip simply moves from one to the other. To test for this possibility, we have used ellipsometry to directly measure the amount of surfactant from either CTAB-only solution or CTAB plus 101 mM KBr solution, each with about 1 h of equilibration. We find that slightly less CTA^+ adsorbs in the presence of 101 mM KBr. Thus, KBr does not cause the adsorption of a second layer under the conditions in which we see the morphological change. Ellipsometry was performed in the absence of an AFM tip, so there is still the possibility that the combined action of KBr and the presence of the tip induces the formation of a second layer. However, it is difficult to conceive how a sharp probe can induce a reproducible pattern of structures on a surface when the pattern is irregular in appearance and covers a much larger area than the tip. We believe that the most likely explanation is that the tip induces a change from cylindrical to "spherical" structure by a pressure increase and/or a volume reduction.

The structural change is reversible. The inset to Figure 4a shows that after the force has exceeded the threshold for the cylinder−sphere transition, the force can be decreased with only a small hysteresis loop. When the force is decreased, the structure reverts to cylindrical. In contrast, when the force is increased beyond the higher-force instability, the behavior is typical of surfactant adsorbates: there is a large hysteresis loop, and the force must be decreased to −2.5 nN to increase the separation discontinuously to 20 nm.

The higher-force transition is shown in Figure 4f. A cross section through a height image captured during the higher-force transition shows that the tip moved 3.6−3.7 nm closer to the mica during the transition. Thus, the tip was more than 3.6 nm above the mica during the top third of the image, a large enough gap to fit a micellar structure.

Figure 4f also shows that the imaged structure is not completely featureless after the second instability. We have observed this behavior for many surfactant systems and conclude that these ill-defined features are probably strongly adsorbed surfactant molecules. Surfactant adsorption isotherms in many systems indicate that at very low concentrations there is already a low density of adsorption.[26] This is believed to be due to specific interactions between the adsorbate and the interface. At higher bulk concentrations further adsorption is believed to occur via lateral interactions between hydrophobic chains. This mechanism implies that desorption of a surface micelle could also be multistep under pressure: first, the "associated" molecules desorb, leaving behind the "proto-micelle", and then the specifically held "proto-micelle" molecules desorb. This mechanism explains why it is common in AFM images to observe the same type of patterning on a surface before and after a mechanical instability. The feature at higher pressure is a template for the aggregate at normal pressure.

Adsorption from CTAB and HBr Solution. The corrosive nature of the HBr solutions (pH 1−3) prevented us from doing any long-term studies of aggregation for these solutions, but we were able to show the existence of slow processes because structures in CTAB/HBr solutions were strongly dependent on whether the mica was first exposed to CTA^+ or to H^+. If CTA^+ was introduced first, then the CTA^+ structure was almost unchanged (see Figure 5a) after 6 h in which the H^+ concentration was increased from $10^{-4.4}$ to 10^{-1} mol L^{-1} (including 2 h at 0.01 M HBr and 30 min at 0.1 M HBr). In fact, the long cylindrical aggregates were imaged with better resolution (possibly because of the shorter decay length of the electrostatic double layer.)

When the mica was pre-equilibrated with H^+, then H^+ had a profound effect on the aggregate structure (Figure 5b and c). At 10 mM H^+, the CTA^+ structure was disrupted in a similar way as for 100 mM K^+; the aggregate axis is aligned over a much shorter distance than in 10 mM K^+ solutions, and there are many more defects. These defects support our hypothesis that adsorbed H^+ ions occupy sites on the mica that could have been used for CTA^+ adsorption, and thus disrupt the ordered arrangement of cylindrical micelles. The higher binding constant of H^+ explains why a lower concentration of H^+ compared to K^+ is required to achieve a similar change.

In H^+ solution, the aggregate axis changed direction more often and more smoothly and was more likely to reverse direction with the net result being swirls and spirals. In contrast, K^+ induced more sudden changes, usually between only two directions. The lumps and the two mechanical instabilities that characterized adsorption in K^+ were also absent. Another feature which distinguished the effect of H^+ from that of K^+ on CTA^+ aggregation was that surface aggregates formed after pre-equilibration with H^+ were more easily perturbed by the action of imaging. The image shown in Figure 5c was captured from the first scan on a previously "untouched" region. Subsequent imaging revealed a structure in which the long axis was more likely to be found normal to the fast scan axis of imaging, analogous to ripples formed in sand by wind or wave action. Straightening of aggregates by imaging is seen at the bottom of Figure 5b.

We were also able to observe features with the aggregate symmetry at forces greater than the instability force in HBr solution. When the instability force was exceeded, the tip moved about 4 nm closer to the mica, but the long, thin structures were still observed. This again shows that there is a more strongly held portion of the aggregate that may be involved in attaching the aggregate to the interface.

Adsorption from CTAB and Tetraethylammonium Bromide Solutions. The structure of the adsorbed

(26) For example, see: *Adsorption from Aqueous Solution*; Weber, W. J., Matijevic, E., Eds.; American Chemical Society: Washington DC, 1968.

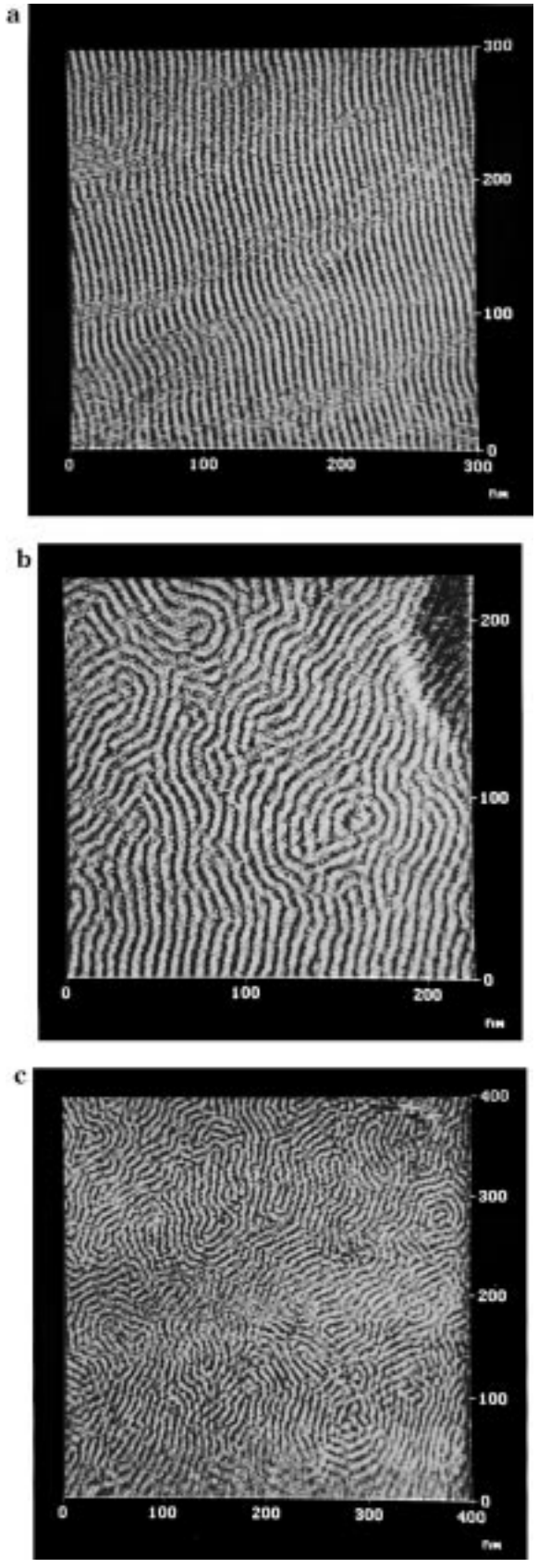

Figure 5. AFM image of the 1.8 mM CTAB/10 mM HBr solution interface. (a) When CTAB is added first, the cylindrical structures are more easily resolved, but otherwise the structure is almost unchanged for 2 h. There is no significant difference when the HBr concentration is increased to 0.1 M for 30 min. b and c When the mica is pre-equilibrated with HBr, the adsorbed structure has many defects, particularly spirals.

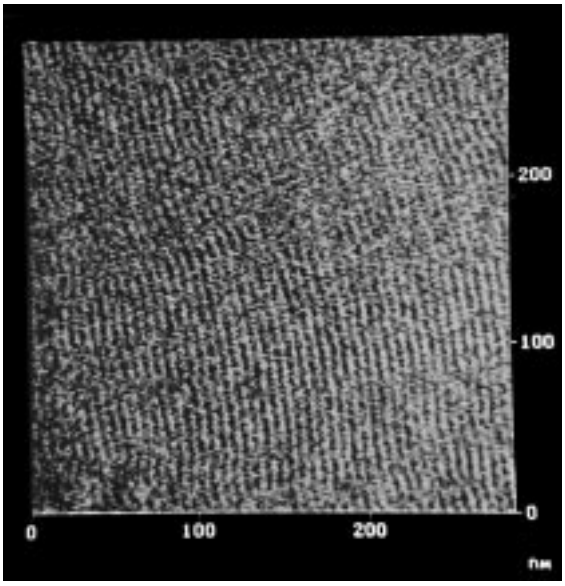

Figure 6. AFM image of the interface between aqueous 1.8 mM CTAB and 100 mM TEAB. The structure was similar for 10 mM TEAB and was the same whether the surface was pre-equilibrated with TEAB or CTAB.

aggregates in the presence of 100 mM tetraethylammonium bromide (TEAB) is shown in Figure 6. The aggregates have far fewer defects than for an equal concentration of KBr or HBr. There was no difference in aggregate structure when the mica was pre-equilibrated with TEAB or with CTAB. Thus, the hydrophobic cation TEA^+ causes less disruption of the aggregates and appears to pass through the surface film more easily than H^+.

Adsorption from Dodecyltrimethylammonium Bromide (DTAB) Solution. In earlier work, we reported that DTAB forms cylinders at the interface between mica and a 2 × cmc solution.[12] Knowing that CTAB changed from cylinders to a flat sheet within 24 h, we re-examined DTAB at the interface between mica and a 2 × cmc DTAB solution over a period of 24 h. The aggregates remained cylindrical for the entire period.

Direction of the Aggregate Axis. In the absence of salt, the long axis of the aggregate points in a single direction over a large area. We have examined the relationship between this direction and the direction of the *b*-axis of mica, as determined from the acute bisectrix interference figure (optical microscopy). For six experiments, the angle was 70°, 90°, 90°, 135°, 165°, and 165°. The error in each measurement is about ±10°. At this stage we can only state that the mica does not dictate a unique aggregate orientation but that the orientation is clustered around two values. In 101 mM KBr, two dominant axis directions are visible in the same image.

Discussion

Relationship between Ion Binding and Aggregate Disruption. The ionic headgroup of CTA^+ drives the initial adsorption to mica and is probably the attachment site of the aggregates. It is reasonable to expect that surface interactions (such as this ionic binding) cause a change from the bulk solution structure. The central hypothesis of this work is that if the binding of the ionic headgroup of CTA^+ dictates substrate-binding and surface-aggregate structure, then competition from other cations should disrupt the organization of adsorbed CTA^+ aggregates. The experimental results support this hypothesis. In the absence of a significant concentration of K^+ (<10 mM), CTA^+ forms a flat layer on mica, because the density of

available binding sites is high (much higher than the equilibrium headgroup spacing in a spherical micelle). The fact that the anions are confined to a plane (the surface of the mica) should also promote the formation of a planar aggregate structure.

Addition of K^+ (>10 mM) leads to a cylindrical structure, then to defective cylinders, and finally to a structure that is spherelike when the AFM tip applies a pressure. With a greater K^+ concentration in solution, more anionic surface sites will be occupied by a rival cation and not available to CTA^+ ions for binding. This means that CTA^+ will either leave the film (our ellipsometry measurements indicate that this occurs to a small extent) or at least detach from the mica and instead bind to Br^-. This makes the adsorbate structure discontinuous. Because the hydrophobic effect leads to clustering of the CTA^+, the discontinuities are not random but are clustered into aggregates. The aggregate structure is then determined by the forces between monomers and those between monomers and the mica sites. In contrast to the micelles in bulk solution at 2 × cmc, the micelles at the surface are in close proximity and should feel relatively strong repulsive electrostatic forces. This should promote alignment of the aggregates. However, the aggregates are still very highly aligned when concentrated HBr (0.1 M) is added after CTAB, and under this condition, the solution side of the aggregates should have a low surface potential. This suggests the alignment is dominated by a force in the mica−aggregate plane. Organization of the cylindrical aggregates by the mica is also supported by the existence of a preferred aggregate orientation relative to the crystal. At high K^+ concentrations, the cylinders have many bends and discontinuities. We suggest that the cause is adsorption of a K^+ ion to a site in the path of the aggregate that forces the aggregate to deviate in direction and attach at another site.

The relationship to the binding constant is also quantitative: the stronger binding H^+ ion has a greater influence per mol L^{-1} than K^+. The dissimilarity in effect of various cation bromides suggests that the cation is the main species affecting the CTA^+ structure.

However, as in bulk solution, we would expect that an increased concentration of anions could also contribute to changes in surface aggregate structure. One can envisage two competing effects: (1) free counterions binding to the surfactant headgroup, decreasing the repulsion between monomers, thus lowering the headgroup area, and (2) free counterions competing with the fixed planar array of surface counterions to allow the aggregate to reach its "free" curvature.

The second effect may be useful in explaining the difference in equilibrium structure for CTAB (flat sheets) and DTAB (cylinders) in the absence of additional salt. It is difficult to explain the two structures with a packing parameter argument.[27] A decrease in hydrocarbon chain length will decrease the hydrocarbon volume, and unless the critical chain length scales with a fractional power, the two effects on the packing parameter will cancel. The surfactants were each imaged at 2 × cmc, but the cmc of DTAB (15 mM) is greater than that for CTAB (0.9 mM), so the free Br^- concentration is much greater in the DTAB solution. This implies a smaller headgroup area and a higher packing parameter for DTAB, a conclusion inconsistent with cylinders for DTAB and a bilayer for CTAB. A possible resolution is that the higher concentration of Br^- in the DTAB solution leads to more binding of DTA^+ to Br^- and less binding of DTA^+ to the mica. The DTA^+ ions are then less confined to the high-density, planar surface sites of the mica and can adopt a shape closer to their "free" solution structure (mechanism 2 above). If this is true, it suggests that the anions make a significant contribution to the bilayer to cylinder transformation when KBr is added to CTAB.

Pressure-Induced Transition. The application of a critical force causes a transformation of surface aggregate structure from cylindrical to spherical in 1.8 mM CTAB and 10 or 101 mM KBr but not in 1.8 mM CTAB solution alone. We can try to rationalize this by taking the ion-exchange hypothesis one step further and assuming that the binding constants are pressure sensitive. Pethica has shown that changes in adsorption density with separation are consistent with previously measured surface forces and with thermodynamic arguments.[28] When the pressure is increased or the volume between the tip and mica is decreased, the smaller K^+ ion should become relatively more favored to bind to mica than the larger CTA^+ ion or the even larger CTAB aggregate. The increased surface concentration of K^+ would then favor the formation of more spherical structures.

Exchange Kinetics. The structure of CTAB on mica is sometimes slow to reach equilibrium. Most of this behavior is consistent with a model in which the thin film of surfactant provides a large barrier to H^+ but not to K^+. The high surface potential in the presence of CTAB (∼150 mV at 0.5 × cmc)[3] will reduce the concentration of cations near the surface, but this electrostatic barrier should be similar for H^+ and K^+. A possible explanation is that the proton has a more difficult passage through the low-dielectric, hydrophobic film because it is harder and more strongly hydrated than K^+. The difference in behavior of H^+ and K^+ is interesting because (a) the apparently discontinuous and exchangeable adsorbed film can provide a barrier and (b) it implies that the surface coating is ion selective.

In CTAB-only solution (at pH 6), there is competition between protons and CTA^+ for surface sites. When the CTAB adsorbs, it must displace H^+, and the results are consistent with the trapping of some H^+ under the film during the initial adsorption of CTAB. The steady state is reached as H^+ leaves the mica surface and passes through the film to the aqueous solution, and additional CTA^+ adsorbs (the model of Chen et al.[9]) Measurements in acidic solution support the idea that the CTA^+ film provides a barrier to passage of protons. The fact that the CTA^+ structure depends on whether the surfactant or the acid is added first suggests that the CTA^+ layer is a barrier to proton passage from solution to the mica surface. A possible reason for this slow equilibration is that the low-dielectric CTA^+ film provides a high activation barrier to passage of the hard, strongly hydrated H^+ ion and also that the energy of CTA^+ or H^+ on the mica site depends on which ions occupy the neighboring sites.

When a large concentration of K^+ is present initially (>10 mM), the film quickly reaches a steady state. Under these circumstances, the mica is mainly neutralized by K^+ and not H^+, suggesting that K^+ is more easily able to penetrate the initially formed surfactant film. The results at 10 mM are not instructive, because the final state is the same as the initial state.

To test the impact of the H^+ to K^+ ratio at the surface when CTAB initially adsorbs, we also performed some experiments where the mica was pre-equilibrated in KOH solution. The mica was cleaved, exposed to 10^{-3} M KOH

(27) Israelachvili, J. N. *Intermolecular and Surface Forces*, 2nd ed.; Academic Press: London, 1992; Chapter 17.

(28) Pethica, B. A. *Colloids Surf.* **1986**, 20, 151−170.

($H^+/K^+ = 1{:}10^8$) for 10 min, exposed to 10^{-3} M KOH and 1.8 mM CTAB for 10 min, and then rinsed with 1.8 mM CTAB to remove the KOH. Thus initial adsorption of CTAB was at low H^+, but the final experimental condition was the same as that in earlier experiments when the mica was exposed to CTAB-only solutions. However, we were unable to resolve faster progression to a steady-state bilayer structure. So far, the only method for speeding the formation of a bilayer has been to raise the temperature.[10]

When H^+ is added after CTAB, it still has little effect even when we image at a sufficient force to displace the CTA^+. This suggests that either the CTA^+ still clings to the mica in a flattened film under the tip (the "protomicelle" concept) or that the CTAB structure can reform rapidly. In the latter mechanism one can envisage the tip moving along the mica surface between surfactant aggregates that bend away in the vicinity of the tip and bend back after the tip moves through. Thus the instability barrier may not be a good measure of the force required to push the surfactant into solution; it may just be the force required for the aggregate to bend locally in the plane of the interface or for part of the micelle to go into solution.

Period Data. The resolution of the AFM image is not high enough to learn much about the cross section of the aggregate, and in particular, interpretation is complicated by the finite size and curvature of the tip. When the tip scans the surfactant aggregates, the tip height typically changes by only ~0.2 nm even though the aggregates are about 4 nm in height. This is probably because the apex of the tip has about the same curvature as the aggregates and so cannot "fit" in the gaps between the aggregates. We can estimate that the tip radius is similar in size to the aggregate diameter because it is possible to image defects in the aggregate structure (e.g. in refs 29−31). However, regardless of the tip geometry, it is still possible to obtain information about the repeat unit of the structures.

The repeat unit, or period, is the sum of the aggregate diameter and the separation. The period of hemicylindrical aggregates of sodium dodecyl sulfate (SDS) on graphite has previously been found to decrease in the presence of added salt, and this was explained in terms of a reduced electrostatic repulsion between the aggregates.[17,32]

We have also collected data for the period of the CTAB aggregates as a function of electrolyte. With the exception of 101 mM KBr, electrolyte did not have a measurable effect on the period in the range 0−101 mM for the monovalent salts investigated. The period remained between 6.5 and 7.1 nm while the Debye length decreased from 7 to 0.9 nm. For 101 mM K^+, the period increased to 7.9 nm, but the measurement error is high because the aggregates are short and the orientation changes rapidly. The lack of effect of electrolyte when the Debye length is in the range of the repeat period implies either that repulsive electrostatic forces do not influence the separation or that another effect cancels out this contribution. Since we measure an electrostatic force normal to the plane of the aggregates, and ionic surfactant aggregates are usually charged, it is likely that there is an electrostatic force between aggregates, so we must look for another influence. There are two possibilities:

(1) The addition of Br^- not only screens the interaggregate repulsions, but it also decreases the repulsion between surfactant molecules within an aggregate. This would cause an increase in aggregate diameter and mitigate the decrease in aggregate separation.

(2) The simultaneous addition of H^+ or K^+ reduces the density of surfactant cation sites and thus the density of surfactant on the mica surface. This cannot be the explanation when H^+ is added after the surfactant, as it does not appear to penetrate the surfactant layer.

Conclusions

At two times the bulk cmc, the shape of CTAB aggregates at the mica surface is affected by the presence of rival cations. In pure CTAB solution, the surfactant forms a flat sheet. Both KBr and HBr transform the flat sheet to cylinders and then defective cylinders with increasing concentration. The inclusion of extra salt into the film can lower the aggregate curvature in two related ways; the cation can occupy attachment sites for CTA^+, and the free anion can bind to CTA^+ in competition with surface anions, thus releasing the aggregate from the planar template with close-packed headgroup-binding sites.

Defects in the cylindrical structure such as termini or deviations in direction are correlated with K^+ and H^+ concentration and may be due to the binding of these ions in the path of the cylinder. The density of defects qualitatively fits a mass action model: more defects occur at a higher K^+ concentration or when H^+ is used instead of K^+. (H^+ is known to bind more strongly to mica).

CTAB films on mica can take a long time to reach a steady-state structure. In 10 mM or greater KBr, the films reach a steady state within minutes, whereas, in the absence of salt or in HBr solutions, the films take hours to reach equilibrium. This suggests that the CTAB layer allows rapid passage of K^+ but not of H^+.

The observed CTAB structure in the presence of K^+ is pressure sensitive. The structure discontinuously changes from defective cylinder to spherelike on the application of pressure.

Acknowledgment. Our thanks go to George Petersen for providing the ultralevers, to Alan Cooper for finding the crystal axis of mica, and to David Beaglehole for performing the ellipsometry.

LA9710942

(29) Jaschke, S.; Butt, H.-J.; Gaub, H. E.; Manne, S. *Langmuir* **1997**, *13*, 1381−1384.
(30) Lamont, R. E.; Ducker, W. A. *J. Colloid Interface Sci.* **1997**, 191, 303−311.
(31) Wanless, E. J.; Davey, T. W.; Ducker, W. A. *Langmuir* **1997**, *13*, 4223−4228.
(32) Wanless, E. J.; Ducker, W. A. *Langmuir* **1997**, *13*, 1463−1474.